An Efficient Coordinate Frame Calibration Method for 3-D Measurement by Multiple Camera Systems

Fei-Yue Wang, *Fellow, IEEE*

***Abstract*—Extrinsic calibration or coordinate frame calibration of multiple cameras is a critical step for conducting three-dimensional measurement effectively from visual images. Based on the concept of relative world coordinate system, an efficient method for calibrating the coordinate frames for multiple cameras has been developed in this paper. Its basic idea is to compute the transformation matrices between cameras from their individual transformation matrices to a relative world coordinate system such that its absolute coordinate information is not required and methods for single camera calibration can be utilized. A solution procedure that separates rotational parameters from translation parameters of transformation matrices has been developed where the rotational parameters are obtained first by solving a set of nonlinear equations involving two Euler angular parameters, while the translational parameters are then calculated analytically. In addition, equations for calculating the depth information and matching lines in general cases have been presented. Finally, a detailed numerical investigation regarding the error and sensitivity analysis of the proposed calibration algorithms has been performed extensively.**

***Index Terms*—Camera calibration, extrinsic parameter calibration, multiple cameras, stereo cameras, three-dimensional (3-D) measurement.**

I. Introduction

CAMERA calibration in computer vision is the process of determining the internal geometric and optical characteristics (intrinsic parameters) and the three-dimensional (3-D) position and orientation of a camera frame relative to a certain world coordinate system (extrinsic parameters) for the purpose of inferring 3-D information from computer image coordinates or computer image coordinates from 3-D information [24]. It is a necessary and critical step for successful applications of computer vision in many real-world problems, ranging from locating objects, targets, or features in measurement or pattern recognition, to calculating the position and orientation of moving cameras in robotics or automation, and to verifying or confirming hypotheses regarding the state of world in assembly or inspection.

Extensive research and experiments on camera calibration have been conducted from the perspective of computer vision and robotic vision over the last two decades. There are two major calibration methods, the photogrammetric calibration that must be performed by observing a calibration object whose geometry in 3-D space is known with high precision, and the self-calibration that can be conducted without the use of any calibration object by moving a camera in a static scene. Major existing photogrammetric calibration technologies include full-scale nonlinear optimization for arbitrarily accurate yet complex imaging models [1], [5], [8], [13], [14], [22], computing perspective transformation matrix using over-determined linear equations [1], [7], [20], [23], [32], two-plane methods [12], [17], [31], and the four-step procedure [24], [10], [11]. Recently, the self-calibration for active vision systems has become the focal point for many research projects in camera calibration [4], [9], [15], [16], [19], [32]. A survey of camera calibration methods and models, especially on historic works, can be found in [3]. Generally, the intrinsic and extrinsic camera parameter calibrations are treated and solved simultaneously in those works.

In this paper, we will exclusively deal with the extrinsic parameter calibration problem for multiple camera systems. Specifically, our problem is to determine the 3-D position and orientation of a camera frame relative to other camera frames for the purpose of inferring 3-D information from computer image coordinates generated by multiple cameras. We are focused on the type of applications where repeated calibration of extrinsic parameters is mandated while the intrinsic parameter calibration needs to be conducted only once. Therefore, it will be assumed that the calibration of intrinsic parameters has been accomplished with the sufficient accuracy and the objective here is to develop an efficient calibration procedure only for extrinsic parameters in multiple camera systems [28].

Such applications can be found in vehicle guidance [2], [21], [27], robotic vision, manufacturing processes, visual security systems, 3-D traffic monitoring, automated 3-D survey of road accident sites, field monitoring systems in mining operations, and motion estimation using airborne camera systems [27]. In those applications, position and orientation of cameras are subject to constant, random and significant disturbances due to motion, thermal effects, environmental variation, or other unpredictable factors, and thus the relative position and orientation among cameras must be calibrated repeatedly for extracting any meaningful 3-D information from computer images. In many cases, such as vehicle guidance and robotic vision, real-time information are critical for successful applications. Therefore, an efficient extrinsic parameter calibration procedure that requires less preparation in setup and computation in processing would be extremely useful in those applications.

Manuscript received August 19, 2003; revised January 8, 2003, April 13, 2004, and September 29, 2004. This work was supported in part by Grants 60125310, 60334020, 2002CB312200, and 030335 from NNSF, MOST, and the Shandong Provincial Government, and in part by a grant from the U.S. Department of Transportation through the ATLAS Research Center at the University of Arizona. This paper was recommended by Associate Editor S. Rubin.

The author is with the The Key Laboratory of Complex Systems and Intelligence Science, Chinese Academy of Sciences, Beijing 100080, China, and also with Department of Systems and Industrial Engineering, University of Arizona, Tucson, AZ 87521 USA.

Digital Object Identifier 10.1109/TSMCC.2004.843208

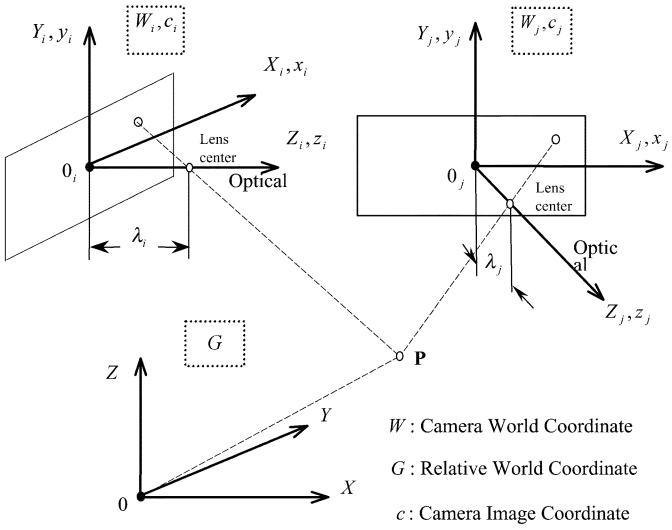

Fig. 1. World and image frames for multiple cameras.

This paper is organized as follows. Section II introduces the basic idea and the corresponding equations for extrinsic parameter calibration of multiple camera systems. The main results of this paper is presented in Section III: The improved calibration equations that requires only relative position information of calibration points, and separates the rotational parameters from the translational parameters of homogeneous transformation matrices between camera coordinate systems. A two-variable approach for solving the calibration equations and its numerical analysis is conducted in Section IV. Equations for 3-D measurement and matching line in general cases are given in Section V. Sensitivity and error analysis to image resolution for digital cameras are performed in Section VI. Finally, Section VII concludes the discussion with suggestions for future work.

II. Basic Idea: The Relative World Coordinate System

Fig. 1 illustrates the basic geometry of the camera model and coordinate frame system. As pointed out earlier, we assume all intrinsic parameters of cameras have been calibrated and the problem here is to calibrate the coordinate frame transformations between cameras for the purpose of 3-D measurement. From Fig. 1, $W_i = (X_i, Y_i, Z_i)^T$ is the 3-D camera coordinate system and $c_i = (x_i, y_i)^T$ is the corresponding image coordinate system for camera i. For the sake of simplicity, we assume camera world and image coordinate axes are identical, Z_i and z_i are the optical axis of camera i and the distance from the center of W_i and c_i to the lens center is equal to the focal length λ_i of camera i.

Image coordinate c_i and world coordinate W_i, are related by [6]

$$c_i = \frac{\lambda_i}{\lambda_i - Z_i} \begin{bmatrix} X_i \\ Y_i \end{bmatrix}, \quad i = 1, 2, \ldots, m. \tag{1}$$

World coordinate W_i and W_j of camera i and j are related by

$$W_i = S_i^j W_j + v_i^j, \quad \text{or} \quad \begin{bmatrix} W_i \\ 1 \end{bmatrix} = H_i^j \begin{bmatrix} W_j \\ 1 \end{bmatrix} \tag{2}$$

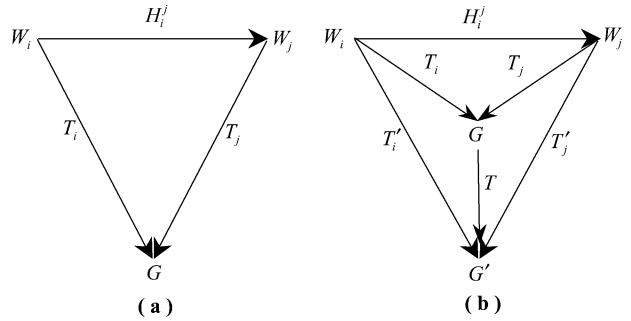

Fig. 2. Relative world coordinate system and camera world coordinate system.

where

$$H_i^j = \begin{bmatrix} S_i^j & v_i^j \\ 0 & 1 \end{bmatrix} \tag{3}$$

is the homogenous transformation between W_i and W_j, S_i^j and v_i^j are rotational matrix and translational vector, representing the relative orientation and position between W_i and W_j, respectively.

The extrinsic calibration problem is to determine transformation matrices $H_i^j, \quad i \neq j, i, j = 1, 2, \ldots, m$ for the multiple cameras system. When $m = 2$, we deal with common stereo camera systems.

To solve this problem, many methods have been proposed [3], [24]. However, most of those methods calibrate either intrinsic parameters specifically or both intrinsic and extrinsic parameters simultaneously. Thus, they are not efficient calibration methods for the type of applications considered in this paper. In our previous effort, we had tried to establish an efficient extrinsic calibration procedure for stereo camera systems based on the concept of a virtual world coordinate system [21], [25]. Here, we improve our previous result by eliminating all absolute position terms from the calibration equations.

Let G be a world coordinate system [see Fig. 2(a)], called the *relative world coordinate system* (RWCS), T_i be the transformation matrix from W_i to G, then it is easy to show that [6]

$$H_i^j = T_i T_j^{-1}, \quad T_i = \begin{bmatrix} R_i & p_i \\ 0 & 1 \end{bmatrix} \tag{4}$$

where R_i and p_i are the corresponding rotation matrix and translation vector, respectively.

Now, we can show that the absolute position and orientation information of RWCS G is not required for calculating H_i^j. To do this, assume G is moved to G', through a transformation T, and T_i' and T_j' are the transformation matrices between W_i and G', W_j and G', respectively [see Fig. 2(b)]. Then

$$T_i' = T_i T, \quad T_j' = T_j T.$$

Therefore

$$H_i^j = T_i'(T_j')^{-1} = (T_i T)(T_j T)^{-1} = T_i T_j^{-1}$$

which indicates that the absolute position and orientation of G is not needed, and only relative information is required.

Based on this idea, one only needs to find T_i and T_j for calculating H_i^j, thus single camera calibration techniques can be used for calibration of multiple cameras system. For example, Wang and Shi [21] have shown that

$$\begin{aligned}
&\lambda_i p_i(1) + x_{i1} p_i(3) - x_{i1}[\lambda_i - R_i(3)G_1] + \lambda_i R_i(1)G_1 = 0\\
&\lambda_i p_i(2) + y_{i1} p_i(3) - y_{i1}[\lambda_i - R_i(3)G_1] + \lambda_i R_i(2)G_1 = 0\\
&\lambda_i p_i(1) + x_{i2} p_i(3) - x_{i2}[\lambda_i - R_i(3)G_2] + \lambda_i R_i(1)G_2 = 0\\
&\lambda_i p_i(2) + y_{i2} p_i(3) - y_{i2}[\lambda_i - R_i(3)G_2] + \lambda_i R_i(2)G_2 = 0\\
&\lambda_i p_i(1) + x_{i3} p_i(3) - x_{i3}[\lambda_i - R_i(3)G_3] + \lambda_i R_i(1)G_3 = 0\\
&\lambda_i p_i(2) + y_{i3} p_i(3) - x_{i3}[\lambda_i - R_i(3)G_3] + \lambda_i R_i(2)G_3 = 0
\end{aligned} \tag{5}$$

where $G_j, j = 1,2,3$ are reference points in RWCS, $G, (x_{ij}, y_{ij})$ is the projection coordinates of G_j in image plane i, and $R_i(j)$ and $p_i(j)$ are jth row of rotation matrix R_i and jth element of translation vector p_i, respectively.

Since these equations are nonlinear for unknown rotational and translation parameters, a closed form solution is difficult to get and a numerical method should be used. However, these equations can be decomposed into two groups. The first group involves only rotational parameters which are nonlinear and should be solved numerically [21]

$$\begin{aligned}
&R_i(3)[x_{i1}(x_{i2} - x_{i3})G_1 + x_{i2}(x_{i3} - x_{i1})G_2\\
&\quad + x_{i3}(x_{i1} - x_{i2})G_3]\\
&\quad - \lambda_i R_i(1)[(x_{i3} - x_{i2})G_1 + (x_{i1} - x_{i3})G_2\\
&\quad + (x_{i2} - x_{i1})G_3] = 0\\
&R_i(3)(x_{i1}y_{i2} - x_{i2}y_{i1})(G_2 - G_1)\\
&\quad - \lambda_i R_i(1)(y_{i1} - y_{i2})(G_2 - G_1)\\
&\quad - \lambda_i R_i(2)(x_{i2} - x_{i1})(G_2 - G_1) = 0\\
&R_i(3)[(x_{i2}y_{i1} - x_{i1}y_{i3})G_1 + x_{i2}(y_{i3} - y_{i1})G_2\\
&\quad + y_{i3}(x_{i1} - x_{i2})G_3]\\
&\quad - \lambda_i R_i(1)(y_{i3} - y_{i1})(G_1 - G_2)\\
&\quad - \lambda_i R_i(2)(x_{i2} - x_{i1})(G_3 - G_1) = 0.
\end{aligned} \tag{6}$$

Using Euler representation for rotation matrix R_i, three Euler angles can be found by solving (6). The next step is to consider (5) as the second group of equations for translation vector only. Since they are linear in terms of p_i, an analytical solution can be found. In theory, we can use three of these equations to find p_i. However, to reduce the noise effects caused by image acquisition and processing, a least square solution has been used. Rewriting (5) in the form $Ap_i = B$, the least solution is given by

$$p_i = (A^T A)^{-1} A^T B.$$

Some detail discussion of the above procedure has been given in [21]. Based on the Newton-Broyden method and numerical simulations, it has been found that: 1) the correct solution for rotational parameters can be obtained as long as the initial guess is within the neighborhood of 30° from the real solution; 2) the selection of $G_0 = (0,0,0)^T$ would lead to large numerical errors in both the rotational and translational parameters [21].

In this paper, we will present an improved version of the above results and a systematic, not *ad hoc*, derivation for calibration equations, show analytically that solution is independent of G_0 selection and the more reference points will lead to a very robust calibration solution with respect to the selection of the initial guess of rotational parameters.

III. Improved Calibration Equations

Let $G_j, j = 0,1,2,3,\ldots,n$ be $(n+1)$ reference points, which are given and defined in the *relative world coordinate system*, and

$$G_j = G_0 + \Delta G_j, \quad \Delta G_0 = 0. \tag{7}$$

Correspondingly

$$\begin{bmatrix} W_{ij} \\ 1 \end{bmatrix} = T_i \begin{bmatrix} G_j \\ 1 \end{bmatrix} \quad \text{or} \quad W_{ij} = R_i G_j + p_i.$$

where W_{ij} is the coordinate of G_j in camera world coordinate system W_i.

Assume the yaw-pitch-roll Euler angles representation for rotation R_i

$$\begin{aligned}
R_i &= \begin{bmatrix} c\theta_2 c\theta_3 & s\theta_1 s\theta_2 c\theta_3 - c\theta_1 s\theta_3 & c\theta_1 s\theta_2 c\theta_3 + s\theta_1 s\theta_3 \\ c\theta_2 s\theta_3 & s\theta_1 s\theta_2 s\theta_3 + c\theta_1 c\theta_3 & c\theta_1 s\theta_2 s\theta_3 - s\theta_1 c\theta_3 \\ -s\theta_2 & s\theta_1 c\theta_2 & c\theta_1 c\theta_2 \end{bmatrix}\\
&= \begin{bmatrix} R_i(1) \\ R_i(2) \\ R_i(3) \end{bmatrix}
\end{aligned} \tag{8}$$

where $(c\theta_i, s\theta_i) = (\cos\theta_i, \sin\theta_i)$, θ_1, θ_2, and θ_3 are yaw, pitch and roll, respectively.

From (1), in terms of rows of the rotation matrix and components of the translational vector, we have

$$\lambda_i p_i(1) + x_{ij} p_i(3) + [\lambda_i R_i(1) + x_{ij} R_i(3)]G_j = \lambda_i x_{ij} \tag{9a}$$

$$\lambda_i p_i(2) + y_{ij} p_i(3) + [\lambda_i R_i(2) + y_{ij} R_i(3)]G_j = \lambda_i y_{ij} \quad i = 1,2,\ldots,m; j = 0,1,\ldots,n. \tag{9b}$$

For any two-point G_j and G_k, we have

$$\begin{aligned}
&\begin{bmatrix} \lambda_i & 0 & x_{ij} \\ 0 & \lambda_i & y_{ij} \\ \lambda_i & 0 & x_{i0} \end{bmatrix} p_i + \begin{bmatrix} (\lambda_i R_i(1) + x_{ij} R_i(3))G_j \\ (\lambda_i R_i(2) + y_{ij} R_i(3))G_j \\ (\lambda_i R_i(1) + x_{i0} R_i(3))G_0 \end{bmatrix}\\
&\quad = \lambda_i \begin{bmatrix} x_{ij} \\ y_{ij} \\ x_{i0} \end{bmatrix}\\
&\begin{bmatrix} \lambda_i & 0 & x_{ik} \\ 0 & \lambda_i & y_{ik} \\ 0 & \lambda_i & y_{i0} \end{bmatrix} p_i + \begin{bmatrix} (\lambda_i R_i(1) + x_{ik} R_i(3))G_k \\ (\lambda_i R_i(2) + y_{ik} R_i(3))G_k \\ (\lambda_i R_i(2) + y_{i0} R_i(3))G_0 \end{bmatrix}\\
&\quad = \lambda_i \begin{bmatrix} x_{ik} \\ y_{ik} \\ y_{i0} \end{bmatrix}
\end{aligned}$$

which leads to (10a) and (10b), shown at the bottom of the page, where

$$u_{ij} = x_{ij}/\lambda_i, \quad v_{ij} = y_{ij}/\lambda_i, \quad \Delta u_{ij} = u_{ij} - u_{i0}$$
$$\Delta v_{ij} = v_{ij} - v_{i0}.$$

Since (10a) and (10b) should lead to the same solution for p_i, we find

$$\Delta v_{ik} R_i(1)(u_{i0}\Delta G_j + \Delta u_{ij}\Delta G_k) - u_{ik}\Delta u_{ij} R_i(2)\Delta G_k + R_i(3)(u_{i0}u_{ij}\Delta v_{ik}\Delta G_j - v_{i0}u_{ik}\Delta u_{ij}\Delta G_k) = 0 \tag{11a}$$

$$v_{ij}\Delta v_{ik} R_i(1)\Delta G_j - \Delta u_{ij} R_i(2)(\Delta v_{ik}\Delta G_j + v_{i0}\Delta G_k) + R_i(3)(u_{i0}v_{ij}\Delta v_{ik}\Delta G_j - v_{i0}v_{ik}\Delta u_{ij}\Delta G_k) = 0 \tag{11b}$$

$$\Delta v_{ik} R_i(1)\Delta G_j - \Delta u_{ij} R_i(2)\Delta G_k + R_i(3)(u_{ij}\Delta v_{ik}\Delta G_j - v_{ik}\Delta u_{ij}\Delta G_k) = 0 \tag{11c}$$

when $j = k$, (11a), (11b), and (11c) lead to the same equation as the following:

$$\Delta v_{ij} R_i(1)\Delta G_j - \Delta u_{ij} R_i(2)\Delta G_j + (u_{ij}\Delta v_{ij} - v_{ij}u_{ij}) R_i(3)\Delta G_j = 0. \tag{12}$$

Using (12) to eliminate $R_i(2)$ in (11a) and $R_i(1)$ in (11b), we arrive at the following set of equations:

$$R_i(1)(\Delta u_{ik}\Delta G_j - \Delta u_{ij}\Delta G_k) + R_i(3)(u_{ij}\Delta u_{ik}\Delta G_j - u_{ik}\Delta u_{ij}\Delta G_k) = 0 \tag{13a}$$

$$R_i(2)(\Delta v_{ik}\Delta G_j - \Delta v_{ij}\Delta G_k) + R_i(3)(v_{ij}\Delta v_{ik}\Delta G_j - v_{ik}\Delta v_{ij}\Delta G_k) = 0 \tag{13b}$$

$$\Delta v_{ik} R_i(1)\Delta G_j - \Delta u_{ij} R_i(2)\Delta G_k + R_i(3)(u_{ij}\Delta v_{ik}\Delta G_j - v_{ik}\Delta u_{ij}\Delta G_k) = 0 \quad i = 1, 2, \ldots, m, \quad j = 1, 2, \ldots, n \tag{13c}$$

which are called the *basic calibration equations for rotational parameters*. Clearly, (13) shows that rotational matrix R_i depends only on the relative information G_j of reference points $G_j, j = 0, 1, 2, \ldots, m$, and particularly, is independent of G_0 selection.

Equation (13) involves three Euler angles, yaw, pitch, and roll; to solve them more effectively, we propose the following algorithm.

1) From the first two equations in (13), solve a linear equation to find

$$A_i \begin{bmatrix} c\theta_i \\ s\theta_i \end{bmatrix} = B_i$$

so that

$$c\theta_i = f_i(\theta_j, \theta_k), \quad s\theta_i = g_i(\theta_j, \theta_k) \quad i \neq j \neq k = 1, 2, 3 \tag{14}$$

where f_i and g_i are the solution from the above linear equation. Equation (14) can be used to find θ_i uniquely since both $c\theta_i$ and $s\theta_i$ are given.

2) Solve the third equation in (13) and following equation for θ_j and θ_k:

$$f_i^2(\theta_j, \theta_k) + g_i^2(\theta_j, \theta_k) = 1. \tag{15}$$

The condition number of A_i can be used to select θ_i among $\theta = \{\theta_1, \theta_2, \theta_3\}$.

Generally, multiple solutions still exist from the proposed calibration algorithm. In this case, additional equations from other reference points can be used to eliminate the false solutions, and make the calibration solution more robust with request to the selection of the initial guess of rotational parameters.

Once rotational parameters have been found, we can use (10a) and (10b) to obtain the translation vector p_i. To reduce the noise effect, we can use the average

$$p_i + R_i G_0 = \frac{1}{2n}\sum_{j=1}^{n}\left(p_{ij}^a + p_{ij}^b\right) \tag{16}$$

where p_{ij}^a and p_{ij}^b are obtained from (10a) and (10b) based on reference point G_j.

Finally, transformation matrices of H_i^j can be found from (4)

$$S_i^j = R_i R_j^T \tag{17}$$

$$v_i^j = p_i - R_i R_j^T p_j = p_i + R_i G_0 - S_i^j(p_j + R_j G_0) = \frac{1}{2n}\sum_{k=1}^{n}\left[\left(p_{ik}^a + p_{ik}^b\right) - S_i^j\left(p_{jk}^a + p_{jk}^b\right)\right] \quad i, j = 1, 2, \ldots, m. \tag{18}$$

Clearly, the above equations indicate that no absolute information is needed for calculating the transformation matrix between any two cameras, only the relative information ΔG is re-

$$\Delta u_{ij}(p_i + R_i G_0) = \begin{bmatrix} u_{i0} R_i(1)\Delta G_j + u_{io}u_{ij} R_i(3)\Delta G_j \\ v_{ij} R_i(1)\Delta G_j - \Delta u_{ij} R_i(2)\Delta G_j + u_{io}v_{ij} R_i(3)\Delta G_j \\ -R_i(1)\Delta G_j - u_{ij} R_i(3)\Delta G_{\mathrm{j}} + \lambda_{\mathrm{i}}\Delta u_{ij} \end{bmatrix} \tag{10a}$$

$$\Delta v_{ik}(p_i + R_i G_0) = \begin{bmatrix} -\Delta v_{ik} R_i(1)\Delta G_k + u_{ik} R_i(2)\Delta G_k + v_{io}u_{ik} R_i(3)\Delta G_k \\ v_{i0} R_i(2)\Delta G_k + v_{io}v_{ik} R_i(3)\Delta G_k \\ -R_i(2)\Delta G_k - v_{ik} R_i(3)\Delta G_{\mathrm{k}} + \lambda_{\mathrm{i}}\Delta v_{ik} \end{bmatrix} \tag{10b}$$

quired, and especially, translation vector is independent of G_0 selection.

A detailed numerical simulation of the improved calibration equation and the proposed solution procedure is given in the following section.

IV. Numerical Analysis of the Proposed Solution Procedure

To show the effectiveness of the improved calibration equation and the proposed two-variable solution procedure, we have conducted extensive numerical analysis with a standard Matlab function *Fminsearch*, a subroutine for multidimensional unconstrained nonlinear minimization based on Nelder-Mead method [18]. Many other more effective methods, such as Newton-Broyden method, are available for solving the basic calibration equation, we select *Fminsearch* due to its wide availability and the convenience to repeat and compare the results.

As the first step, we can easily find A_i and B_i, shown in the equation at the bottom of the page, where a_{ij}, b_{ij}, e_{ij} are the corresponding constants that can be determined from (13a) and (13b).

In general, the condition number of A_i can be used to select θ_i. When the condition numbers are all reasonable, we should choose the variable with the least knowledge regarding its real value. However, we will take $i = 1$, i.e., yaw as θ_i in our simulation here. In order to maintain the orthogonality of the rotation matrix, once θ_j and θ_k have been solved, θ_i will be calculated as

$$\cos\theta_i = f_i/\sqrt{f_i^2 + g_i^2}, \quad \sin\theta_i = g_i/\sqrt{f_i^2 + g_i^2}.$$

The following numerical values and parameters are used.

Calibration Points:

$G_0 = [1 \quad 1 \quad 2]^T$ cm, $\quad G_1 = [16 \quad 11 \quad 37]^T$ cm

$G_2 = [6 \quad 41 \quad 17]^T$ cm, $\quad G_3 = [11 \quad 26 \quad 22]^T$ cm.

Parameters for Camera 1 :

$\lambda_1 = 35$ mm, $\Theta_1 = [45^\circ, 30^\circ, 60^\circ]$

$p_1 = [20 \quad 10 \quad 300]^T$ cm.

Parameters for Camera 2:

$\lambda_2 = 20$ mm, $\Theta_2 = [40^\circ, 35^\circ, 70^\circ]$

$p_2 = [25 \quad 15 \quad 250]^T$ cm.

Parameters for Fminsearch:

$\text{MaxFunEvals} = 100000, \text{TolFun} = 10^{-6}$

$\text{TolX} = 10^{-4}$.

In all computations, the total calibration equation residual and parameter error are defined and measured by

$$e_r = |\text{residual of (13c)}| + |\text{residual of (15)}|$$
$$e_\theta = ||\Theta - \Theta_{\text{real}}||.$$

In sequel, we discuss the sensitivity to initial guesses for three-point calibration versus four-point calibration, two-variable solution procedure versus three-variable solution procedure, as well as the sensitivity to the depth variation.

A. Three-Point Versus Four-Point Calibrations

Figs. 3 and 4 indicate the sensitivity of the two-variable solution to initial guesses for the three-point and four-point calibration, respectively, where "+" at (θ_j, θ_k) represents a correct solution has been obtained $(e_r < 10^{-4}, e_\theta < 10^{-4})$, "×" a false solution $(e_r < 10^{-4}, e_\theta > 10^{-4})$, "0" no solution $(e_r > 10^{-4}, e_\theta > 10^{-4})$, and "∗" the real solution. For camera 1 [Fig. 3(a) and (b)], the three-point calibration obtains 23 correct solutions, seven false solutions, while the four-point calibration leads to 30 correct solutions, no false solution. For example, initial guess (10°, 90°) leads to a final solution (48.29°, 118.61°) with a calibration residual $e_r = 1.3 \times 10^{-6}$ for three-point calibration with G_0, G_1, G_2. Similar result is found for camera 2 (Fig. 4). Clearly, four-point calibration leads to a more robust solution and is better than three-point calibration.

B. Three-Variable Versus Two-Variable Solution Procedures

Fig. 5 shows the sensitivity of the three-variable solution procedure to initial guesses for camera 1, with four-point calibration. Comparing with Fig. 3(b), as we would expect intuitively, when the initial guess for yaw (θ_1) is close to its actual value, the three-variable solution procedure is better than the two-variable solution procedure [47 versus 30 correct solutions, see Fig. 5(a)], while when the initial guess is far from its real value, the three-variable procedure is far worse

$$A_1(\theta_2,\theta_3) = \begin{bmatrix} a_{13}s_2c_3 - a_{12}s_3 + e_{13}c_2 & a_{12}s_2c_3 + a_{13}s_3 + e_{12}c_2 \\ b_{12}c_3 + b_{13}s_2s_3 + e_{23}c_2 & b_{12}s_2s_3 - b_{13}c_3 + e_{22}c_2 \end{bmatrix}$$

$$B_1(\theta_2,\theta_3) = \begin{bmatrix} e_{11}s_2 - a_{11}c_2c_3 \\ e_{21}s_2 - b_{11}c_2s_3 \end{bmatrix}$$

$$A_2(\theta_3,\theta_1) = \begin{bmatrix} a_{11}c_3 + e_{12}s_1 + e_{13}c_1 & a_{12}s_1c_3 + a_{13}c_1c_3 - e_{11} \\ b_{11}s_3 + e_{22}s_1 + e_{23}c_1 & b_{12}s_1s_3 + b_{13}c_1s_3 - e_{21} \end{bmatrix}$$

$$B_2(\theta_3,\theta_1) = \begin{bmatrix} a_{12}c_1s_3 - a_{13}s_1s_3 \\ b_{13}s_1c_3 - b_{12}c_1c_3 \end{bmatrix}$$

$$A_3(\theta_1,\theta_2) = \begin{bmatrix} a_{11}c_2 + a_{12}s_1s_2 + a_{13}c_1s_2 & a_{13}s_1 - a_{12}c_1 \\ b_{12}c_1 - b_{13}s_1 & b_{11}c_2 + b_{12}s_1s_2 + b_{13}c_1s_2 \end{bmatrix}$$

$$B_3(\theta_1,\theta_2) = \begin{bmatrix} e_{11}s_2 - e_{12}s_1c_2 - e_{13}c_1c_2 \\ e_{21}s_2 - e_{22}s_1c_2 - e_{23}c_1c_2 \end{bmatrix}$$

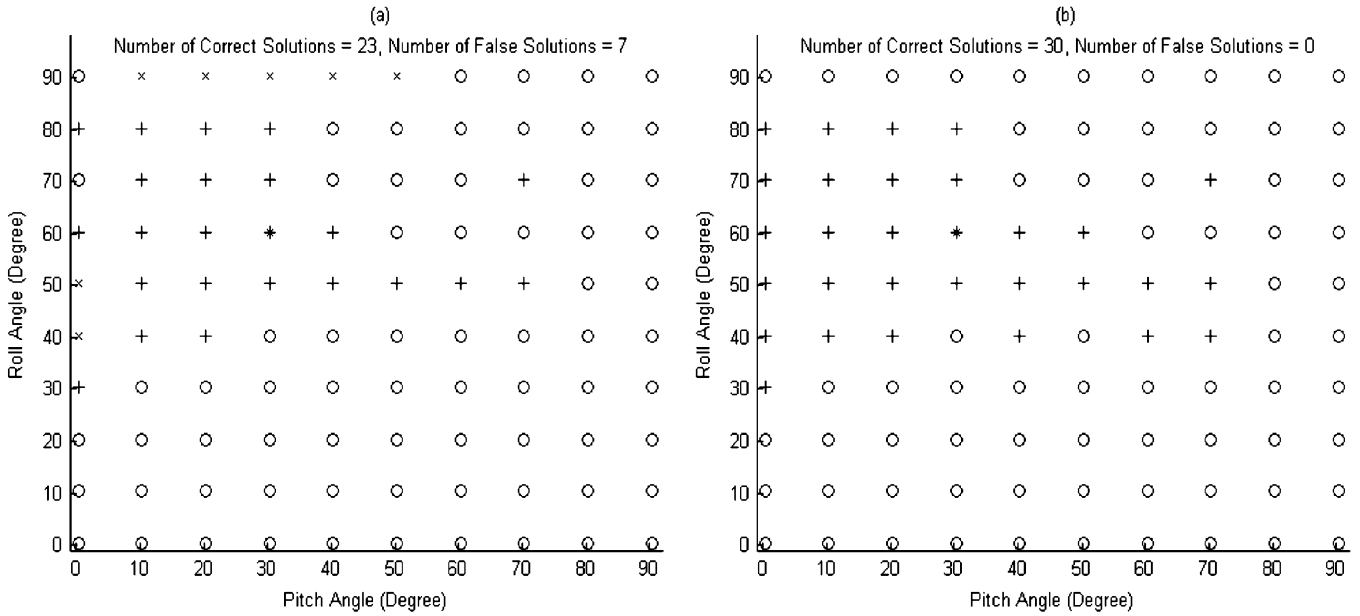

Fig. 3. Sensitivity to initial guesses for camera 1. (a) Three-point calibration for camera 1. (b) Four-point calibration for camera 1.

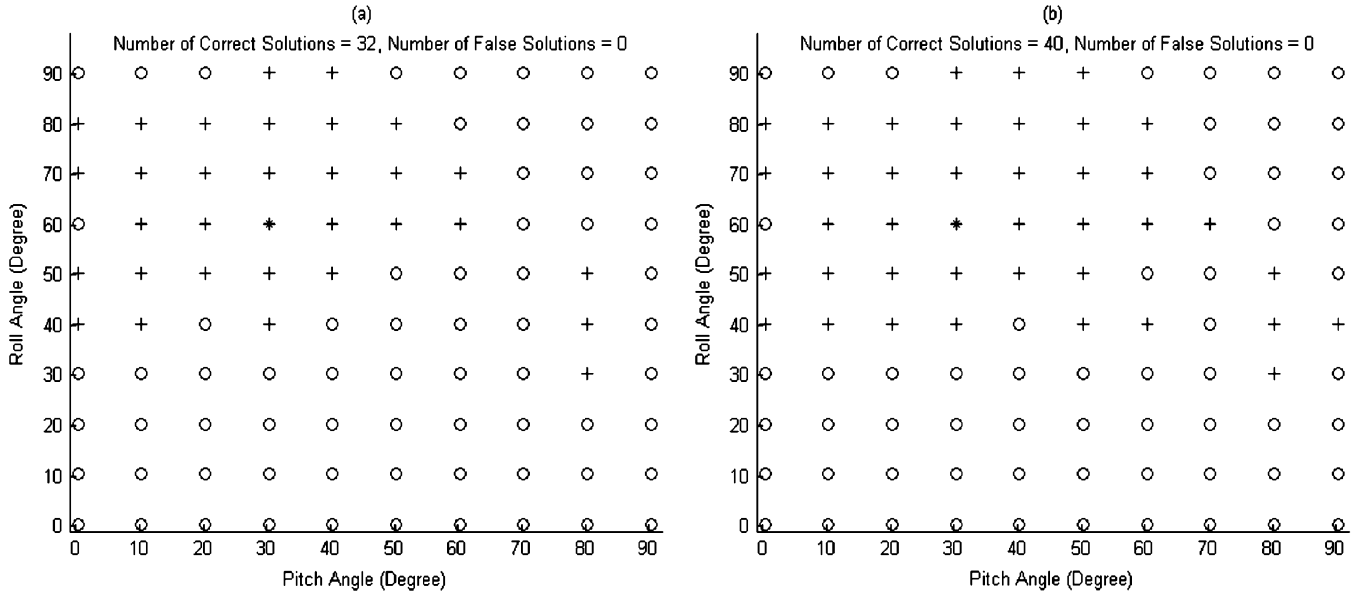

Fig. 4. Sensitivity to initial guesses for camera 2. (a) Three-point calibration for camera 2. (b) Four-point calibration for camera 2.

than the two-variable one [11 versus 30 correct solutions, 5 versus 0 false solution; see Fig. 5(b)]. However, in both cases the three-variable procedure takes more computing time to produce a solution than the two-variable procedure does. Since we should choose another parameter as θ_1 when we have a good guess of yaw, the two-variable solution procedure should obtain results better than the three-variable procedure.

C. Sensitivity to Depth Variation

To investigate the sensitivity of the calibration solution to variation in how far the calibration points are from the cameras, we vary the distance of calibration point G_0 to camera 1 from 20 to 320 cm. We find almost no changes in the convergence of the calibration solution. As one can see from Fig. 6(a) and (b), calculated from initial guess $(\theta_2, \theta_3) = (15°, 30°)$, there are virtually no changes in the calibration equation residual [all have the order of 10^{-14}; see Fig. 6(a)], and rotational parameter error [all have the order of 10^{-13}; see Fig. 6(b)], for both three-point and four-point calibration method. This result is a natural consequence of our improved calibration equation and is quite different from the observation described in [21].

V. Recovering 3-D Information From Multiple Cameras

Once the homogeneous transformation between W_i and W_j is determined, one will be able to find 3-D information of objects in the common view field of two camera i and j, respect to their own world coordinate systems. For example, if cameras i and j are perfectly aligned and form a stereo camera with a baseline

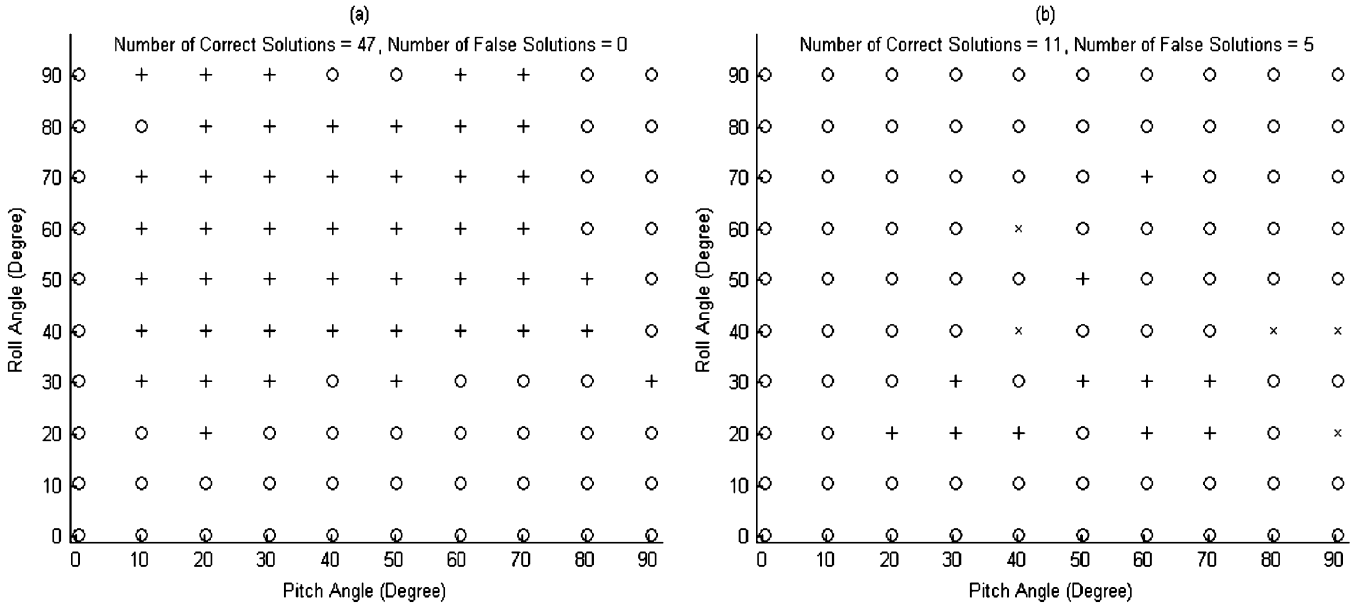

Fig. 5. Sensitivity to initial guesses for three-variable solution procedure. (a) Three-variable solution procedure: Initial $\mathrm{Y_{aw}} = 40$ degree. (b) Three-variable solution procedure: Initial $\mathrm{Y_{aw}} = 10$ degree.

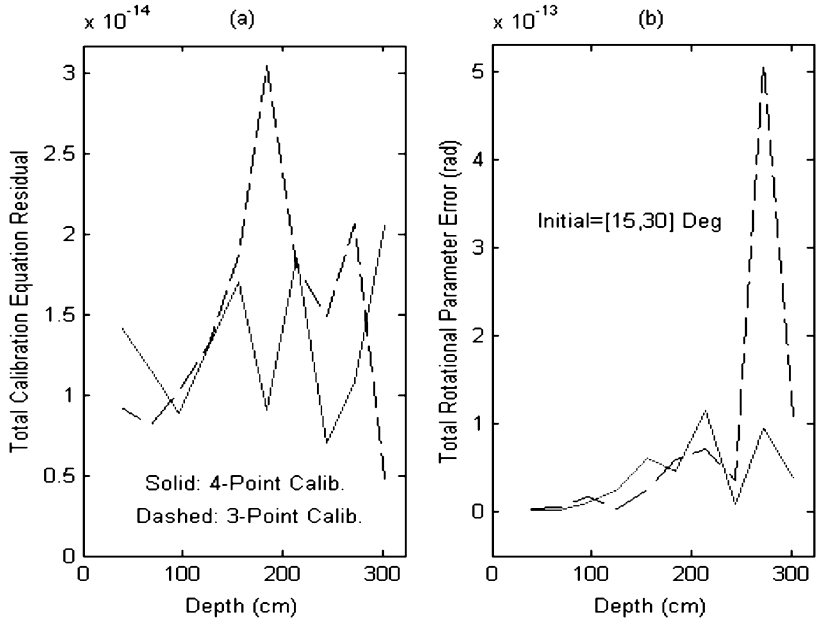

Fig. 6. Calibration residual and solution error versus depth variation.

B (the distance between the centers of the lenses; see Fig. 7), then [6]

$$R_i^j = I_{3\times 3}, \quad p_i^j = (B \quad 0 \quad 0)^T$$

and

$$Z_i = Z_j = \lambda_i \left(1 - \frac{B}{x_i - x_j}\right) \tag{19}$$

$$\begin{pmatrix} X_i \\ Y_i \end{pmatrix} = \left(1 - \frac{Z_i}{\lambda_i}\right) c_i. \tag{20}$$

In the general case, rewrite rotation matrix and translation vector as

$$S_i^j = \begin{bmatrix} \Phi & \alpha \\ \beta & \gamma \end{bmatrix}, \quad p_i^j = [u \quad w]^T \tag{21}$$

where Φ is a 2×2 matrix, α, β^T, and u are 2×1 vector, γ and w are two scalars. Then, (1) and (2) lead to the following equations with respect to depth information Z_i and Z_j

$$c_i \left(1 - \frac{Z_i}{\lambda_i}\right) = \Phi c_j \left(1 - \frac{Z_j}{\lambda_j}\right) + \alpha Z_j + u \tag{22}$$

$$Z_i = \beta c_j \left(1 - \frac{Z_j}{\lambda_j}\right) + \gamma Z_j + w. \tag{23}$$

Therefore, we find

$$\phi_{ij} Z_i = a_{ij}, \quad \phi_{ij} Z_j = b_{ij}$$

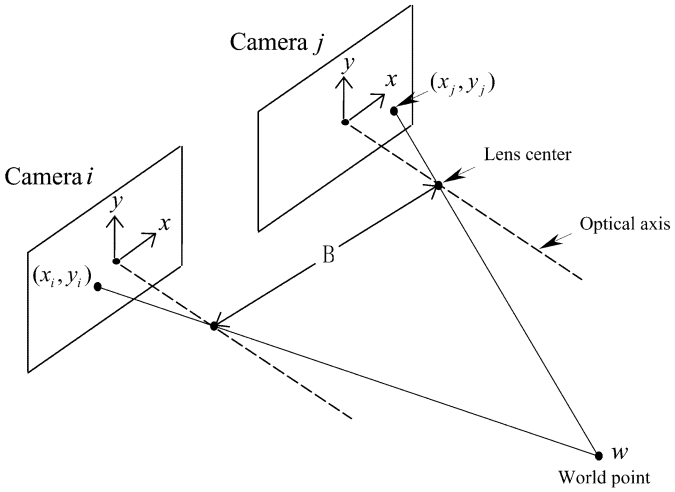

Fig. 7. Stereo camera model.

where

$$\begin{aligned}\phi_{ij} &= \alpha - \Phi d_j + (\gamma - \beta d_j)d_i \\ a_{ij} &= w(\alpha - \Phi d_j) - u(\gamma - \beta d_j) \\ &\quad + \lambda_i(\gamma - \beta d_j)d_i + \lambda_j(\alpha\beta - \gamma\Phi)d_j \\ b_{ij} &= (\lambda_i - w - \lambda_j\beta d_j)d_i - u - \lambda_j\Phi d_j \\ (c_i, c_j) &= (\lambda_i d_i, \lambda_j d_j)\end{aligned}$$

are 2×1 vectors.

Considering the noise effect, we can use the least square solution for calculating depth

$$Z_i = \frac{1}{m-1}\sum_{j\neq i}^{m}\frac{\phi_{ij}^T a_{ij}}{\phi_{ij}^T\phi_{ij}}. \tag{24}$$

A similar solution can be found for other cameras. Note that, in order to find the 3-D information with respect to RWCS G, we must know G_0. For a stereo camera, the above equation reduces to (19).

Actually, one can solve for depth information Z_i and Z_j from (22) only, i.e.

$$[Z_i \quad Z_j]^T = \begin{bmatrix}\frac{c_i}{\lambda_i} & \alpha - \frac{c_j}{\lambda_j}\end{bmatrix}^{-1}(c_i - \Phi c_j - u)$$

and after eliminating Z_i and Z_j from (23), one arrives at the following equation:

$$\begin{bmatrix}1 & \beta\frac{c_j}{\lambda_j} - \gamma\end{bmatrix}\begin{bmatrix}\frac{c_i}{\lambda_i} & \alpha - \frac{c_j}{\lambda_j}\end{bmatrix}^{-1}(c_i - \Phi c_j - u) = \beta c_j + w. \tag{25}$$

The above (25) implies a constraint between image c_i and c_j, therefore they are not independent. Given c_j and expending (25), one find the following linear equation:

$$[A \quad B]d_i = C \tag{26}$$

where $d_i = c_i/\lambda_i$, and

$$\begin{aligned}A &= b_1 - a_3b_2 - b_1b_3; \quad B = a_1b_3 + a_2a_3 - a_1; \\ C &= a_2b_1 - a_1b_2 \\ [a_1, b_1]^T &= \alpha - c_j/\lambda_j; \quad [a_2, b_2]^T = (\Phi c_j + u)/\lambda_i; \\ [a_3, b_3]^T &= [\beta c_j/\lambda_j - \gamma \quad (\beta c_j + w)/\lambda_i].\end{aligned}$$

Therefore, all image points c_i corresponding to image point c_j lies on a straight line defined by (26). This constraint would be useful in matching image points of world points on multiple cameras. It reduces the matching process from a two dimensional searching problem to a one dimensional searching problem.

VI. Error and Sensitivity Analysis for Digital Images

The results described in the previous sections are all based on perfect analog images. However, in the actual applications, most cameras are digital ones and image will be digitized into discrete pixels. Therefore, we will investigate the effect of digital resolution on the sensitivity and accuracy of calibration solution, and the corresponding error in 3-D measurement in this section.

A. Effect on Sensitivity to Initial Guesses

Fig. 8 shows the effect of digital resolution on the sensitivity to initial guesses for camera 1 with an image of size 1×1 in (2.54×2.54 cm) and digital resolution of 512×512 pixels. The corresponding results for a perfect analog image are given in Fig. 3. However, $e_r = 0.01$ and $e_\theta = 4$ degrees are used to classify correct, false and no solution in this case. Therefore, Figs. 3 and 8 can not be compared directly. Clearly, for digital images, the four-point calibration is still much better than the three-point calibration (the number of correct solution increases to 31 from 26, while the number of false solution reduces to 10 from 15, from the four-point to three-point calibration); see Fig. 8(a) and (b). Fig. 9 presents the percentages of correct and false solutions when digital resolutions change from 32×32 to 1024×1024 pixels, numerical results indicate both percentages are stable for digital resolution higher than 500×500 pixels.

B. Effect on Calibration Accuracy

Fig. 10 presents the effect of digital resolution on the calibration accuracy for rotational parameters, while Fig. 11 gives the corresponding results for translational parameters. Initial guess of $[\theta_2, \theta_3] = [20°, 40°]$ has been used in those calculations. Three different depths have been used to include the depth effect. Both figures indicate that the accuracies are stabilized after a digital resolution of 500×500 pixels, while the close distances to the camera along the optical axis will result in a better accuracy for calibration equations, rotational and translation parameters.

C. Effect on Measurement Errors

Fig. 12 shows the effect of digital resolution on the measurement accuracy. Equations developed in Section V have been used to calculate depth information Z and total position information $[X, Y, Z]^T$ for four calibration points. Fig. 12 gives the

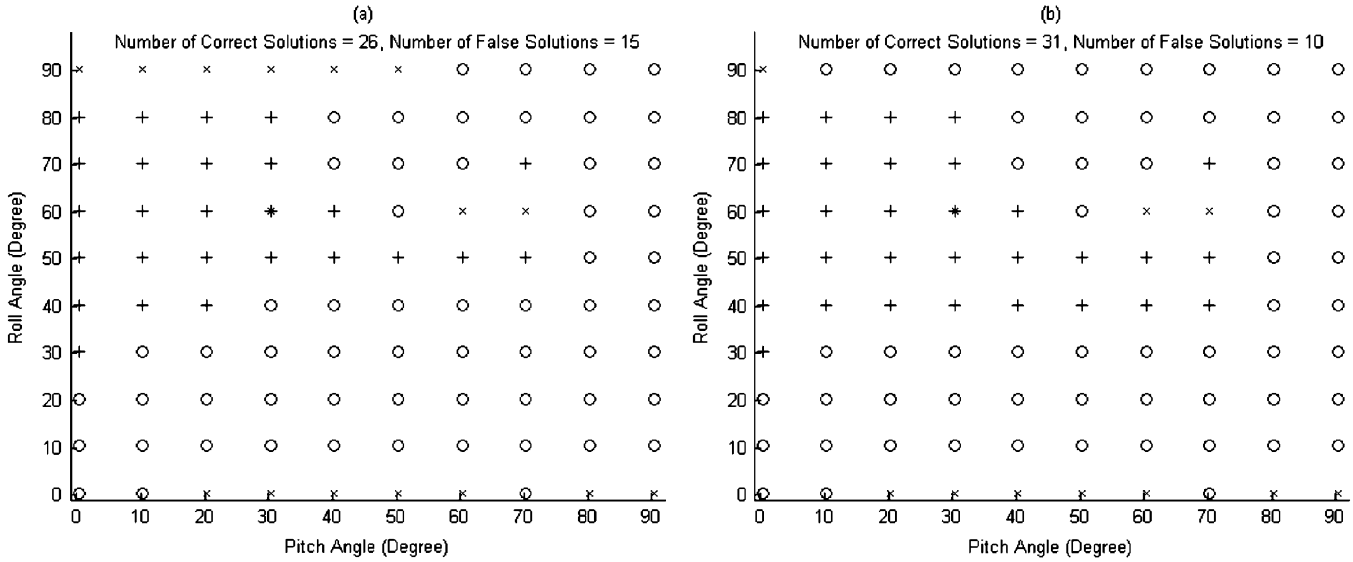

Fig. 8. Sensitivity to initial guesses for digital camera (512 × 512 Rresolution). (a) Three-point calibration for 512 × 512 resolution. (b) Four-point calibration for 512 × 512 resolution.

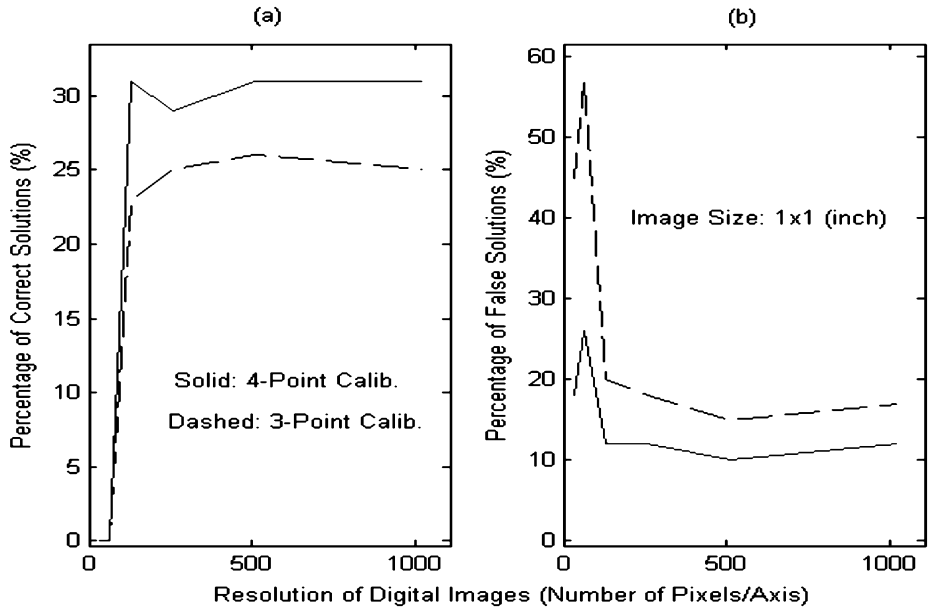

Fig. 9. Correct and false solution versus digital resolution.

average depth and position errors for camera 1 and 2, when resolution changes from 32×32 to 1024×1024 pixels for three different depths of G_0 ($Z_0 = 301, 213, 96$ cm with respect to camera 1). From those figures, the depth and total position errors behave very similar, but actual numerical values are different. As before, the results are stabilized after resolution has reached 500×500 pixels, and the closer to cameras, the better the accuracy.

In general cases, the effect of rotation parameter errors on the measurement accuracy can be measured using the maximum eigenvalue of the difference in rotation matrix. This can be seen from (2) and (4)

$$\Delta W_i = \Delta S_i^j W_j + \Delta v_i^j \quad \text{or} \quad \Delta W_i = \Delta R_i G + \Delta p_i.$$

Thus

$$\begin{aligned} \|\Delta W_i\| &\le \left\|\Delta S_i^j W_j\right\| + \left\|\Delta v_i^j\right\| \le \left\|\Delta S_i^j\right\| \|W_j\| + \left\|\Delta v_i^j\right\| \\ &\le \lambda_{\max}^S \|W_j\| + \left\|\Delta v_i^j\right\| \quad \text{or} \quad \|\Delta W_i\| \\ &\le \lambda_{\max}^R \|G\| + \|\Delta p_i\| \end{aligned}$$

where $\lambda_{\max}^S$ and $\lambda_{\max}^R$ are the maximum eigenvalue of rotation matrix differences ΔS_i^j and ΔR_i, respectively.

Fig. 13(a) shows the changes of maximum eigenvalue for the rotation matrix from camera 1 to RWCS G, while Fig. 13(b) shows the corresponding results for the rotation matrix from camera 1 to camera 2, for three different depths from G_0 to camera 1.

Finally, Fig. 14 presents the effect of digital resolutions on the matching lines on camera 1 for two image points $d_1 =$

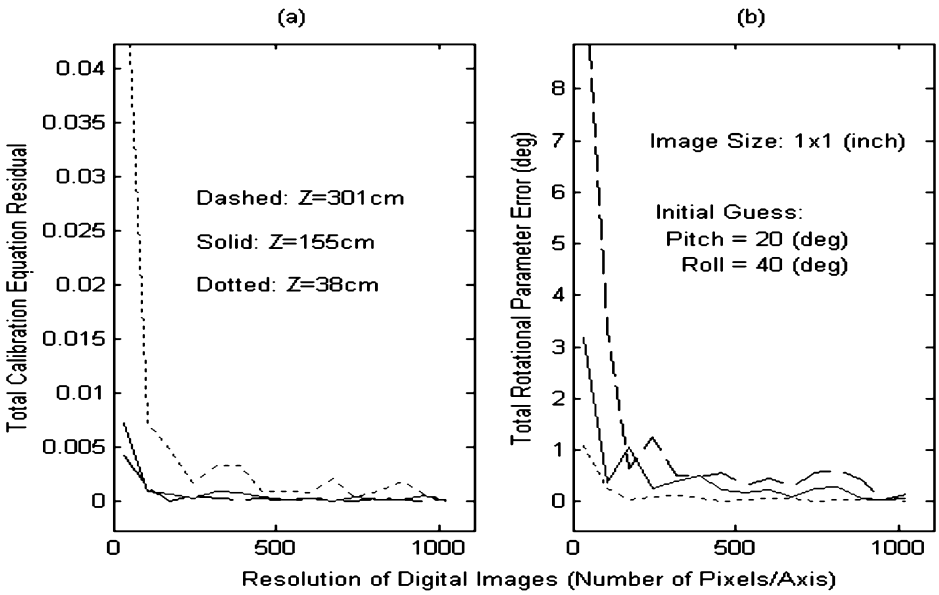

Fig. 10. Calibration accuracy and rotational parameter error versus digital resolution.

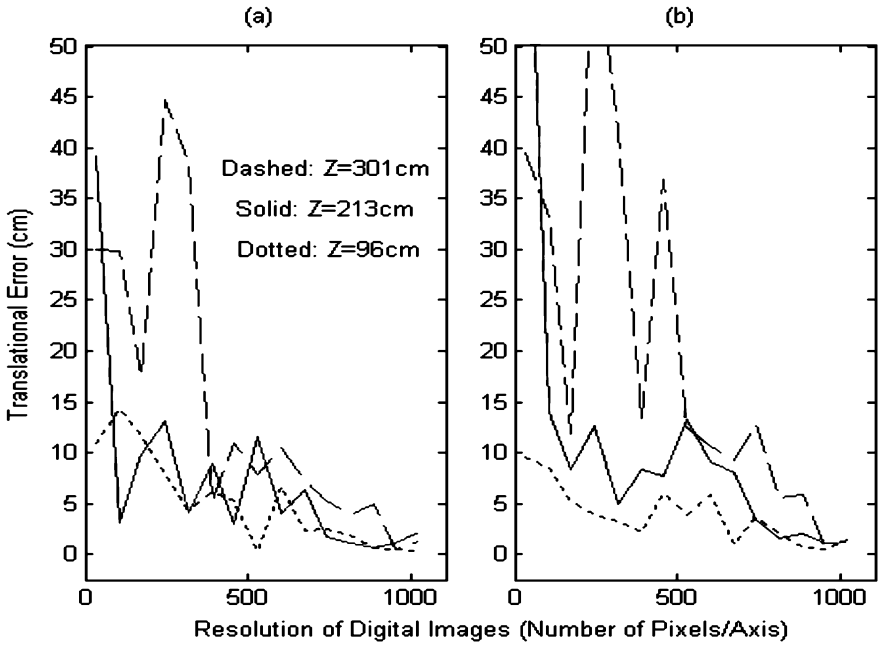

Fig. 11. Translational parameter error versus digital resolution. (a) Camera 1 to RWCS. (b) Camera 1 to Camera 2.

$(0.381, 0.572)$ and $d_2 = (-0.127, -0.254)$, respectively. It is calculated by considering both calibration error and digitization error. Again, it indicates that for a resolution higher than 500×500 pixels, the matching line will be stabilized.

VII. Conclusions and Future Work

An improved calibration equation for extrinsic parameter calibration of multiple camera systems has been developed in this paper. Based on the concept of a relative world coordinate system, the improved calibration equation requires no absolute position information of calibration points and separates the rotational parameters from the translational parameters of homogeneous transformation matrices between camera coordinate systems. A two-variable, instead of the commonly used three-variable, numerical procedure for solving the calibration equations has been proposed and its efficiency is demonstrated through extensive numerical analysis. Equations for 3-D measurement in general cases have also been given in this paper. Sensitivity and error analysis to image resolution for digital cameras have been conducted in details and results indicate the overall benefit of the improved calibration procedure.

Note that Matlab *Fminsearch* has been used exclusively for all numerical analysis in this paper. We would like to emphasize that its use is based purely on the consideration of convenience and availability, and more effective methods must be used in real

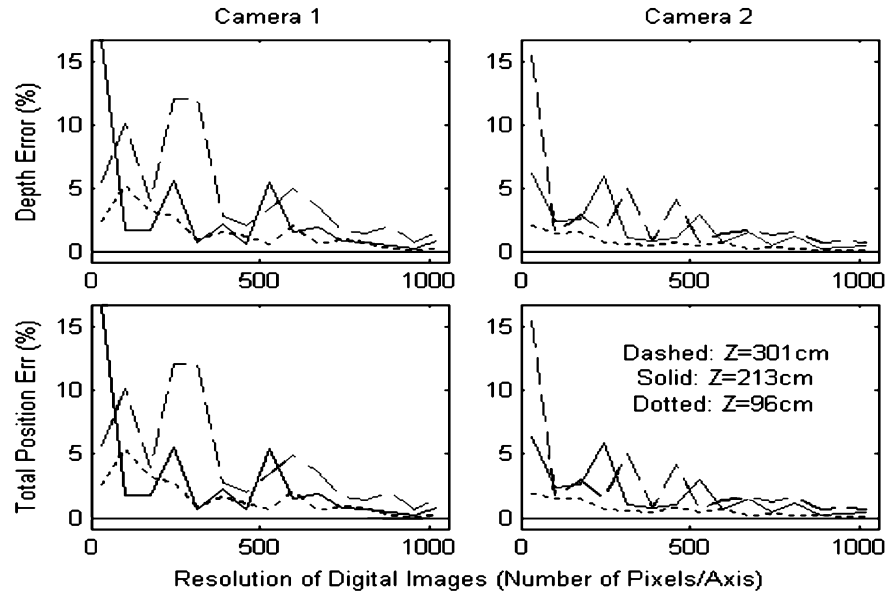

Fig. 12. Position measurement error versus digital resolution.

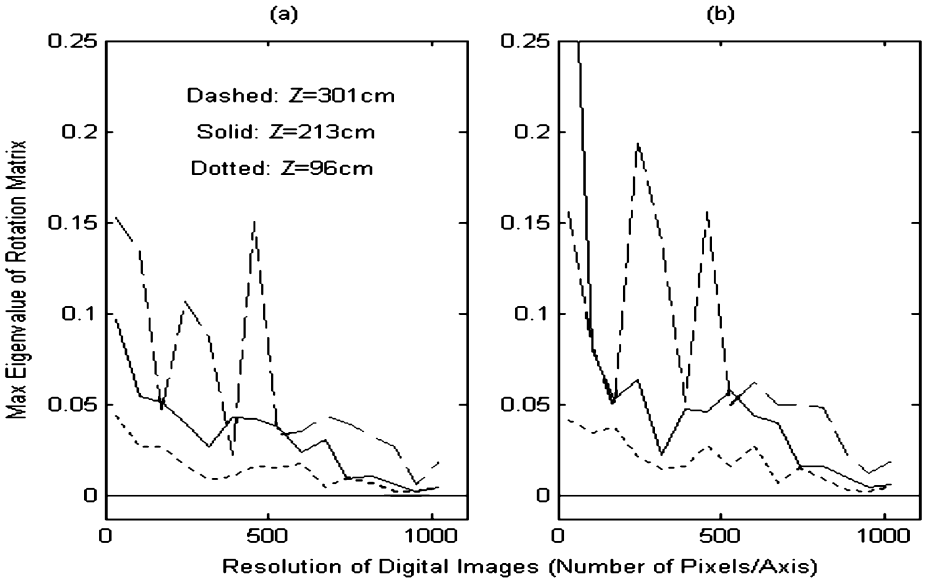

Fig. 13. Max eigenvalue of rotation matrix versus digital resolution. (a) Camera 1 to RWCS. (b) Camera 1 to Camera 2.

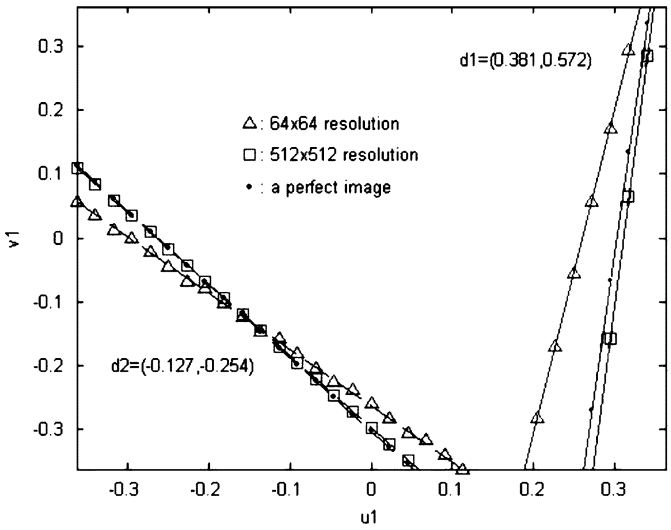

Fig. 14. Variation of matching lines versus digital resolution.

applications. New calibration equation solver and consideration of real-time re-calibration will be the focus of our future investigation.

REFERENCES

[1] Y. I. Adbel-Aziz and H. M. Karara, "Direct linear transformation into object space coordinates in close-range photogrammetry," in *Proc. Symp. Close-Range Photogrammetry*, Urbana, IL, 1971, pp. 1–18.

[2] A. Broggi, M. Bertozzi, A. Fascioli, and G. Conte, *Automatic Vehicle Guidance: The Experience of the ARGO Autonomous Vehicle*. Singapore: World Scientific, 1999.

[3] T. A. Clarke and J. G. Fryer, "The development of camera calibration methods and models," *Photogramm. Rec.*, vol. 16, no. 91, pp. 51–66, Apr. 1998.

[4] R. S. Enciso and T. Vieville, "Self-calibration from four views with possibly varying intrinsic parameters," *Image Vis. Comput.*, vol. 15, pp. 293–305, 1997.

[5] W. Fiag, "Calibration of close-range photogrammetry systems: Mathematical formulation," *Photogramm. Eng. Remote Sens.*, vol. 41, pp. 1479–1486, 1975.

[6] K. S. Fu, R. C. Gonzalez, and C. S. G. Lee, *Robotics: Control, Sensing, Vision, and Intelligence*. New York: McGraw-Hill, 1987.
[7] S. Ganapaphy, "Decomposition of transformation matrices for robot vision," in *Proc. Int. Conf. Robotics and Automation*, 1984, pp. 130–139.
[8] D. B. Gennery, "Stereo-camera calibration," in *Proc. Image Understanding Workshop*, pp. 101–108.
[9] R. I. Hartley, "Self-calibration of stationary cameras," *Int. J. Comput. Vis.*, vol. 22, no. 1, pp. 5–23, 1997.
[10] J. Heikkilä and O. Silvén, "A four-step camera calibration procedure with implicit image correction," in *IEEE Computer Society Conf. Computer Vision and Pattern Recognition*, San Juan, PR, 1997, pp. 1106–1112.
[11] ——, "Geometric camera calibration using circular control points," *IEEE Trans. Pattern Anal. Mach. Intell.*, vol. 22, no. 10, pp. 1066–1077, Oct. 2000.
[12] A. Isaguirre, P. Pu, and J. Summers, "A new development in camera calibration: Calibration a pair of mobile cameras," in *Proc. Int. Conf. Robotics and Automation*, 1985, pp. 74–79.
[13] R. K. Lens and R. Y. Tsai, "Techniques for calibration of scale factor and image center for high accuracy 3-D machine vision metrology," in *Proc. IEEE Int. Conf. Robotics and Automation*, Raleigh, NC, Mar. 31–Apr. 3, 1987.
[14] J. Y. Luh and J. A. Klaasen, "A three-dimension vision by off-shelf system with multi-cameras," *IEEE Trans. Pattern Anal. Mach. Intell.*, vol. PAMI-7, no. 1, pp. 35–45, Jan. 1985.
[15] Q.-T. Luong and O. D. Faugeras, "Self-calibration of a moving camera from point correspondences and fundamental matrices," *Int. J. Comput. Vis.*, vol. 22, no. 3, pp. 261–289, 1997.
[16] S. De Ma, "A self-calibration technique for active vision systems," *IEEE Trans. Robot. Automat.*, vol. 12, no. 1, pp. 114–120, Feb. 1996.
[17] H. A. Martins, J. R. Birk, and R. B. Kelly, "Camera models based on data from two calibration planes," *Comput. Graph. Image Process.*, vol. 17, pp. 173–180, 1981.
[18] [Online]. Available: http://www.mathworks.com/access/helpdesk/help/toolbox/optim/fminsearch.shtml
[19] S. J. Maybank and D. Olivier, "A theory of self-calibration of a moving camera," *Int. J. Comput. Vis.*, vol. 8, no. 2, pp. 123–151, 1992.
[20] R. Samtaney, "A method to solve interior and exterior camera calibration parameters for image resection," NASA Ames Research Center, Tech. Rep. NAS-99-003, Apr. 1999.
[21] X. Shi and F.-Y. Wang, "Basics of binocular stereo computer vision for autonomous rock excavation," in *Autonomous Rock Excavation: Intelligent Control Techniques and Experimentation*. Singapore: World Scientific, 1998.
[22] I. Sobel, "On calibrating computer controlled cameras for perceiving 3-D scenes," *Artif. Intell.*, vol. 5, pp. 185–188, 1974.
[23] T. M. Strat, "Recovering the camera parameters from a transformation matrix," in *Proc. DARPA Image Understanding Workshop*, Oct. 1984, pp. 264–271.
[24] R. Y. Tsai, "A versatile camera calibration technique for high accuracy 3D machine vision metrology using off-the-shelf TV cameras and lenses," in *IBM RC 11413*, Oct. 1985.
[25] F.-Y. Wang, "On the extrinsic parameter calibration for stereo cameras," in *Proc. Int. Conf. Intelligent Manufacturing*, Wuhan, China, 1995, pp. 145–151.
[26] F.-Y. Wang and P. B. Mirchandani, "On estimation of real-time traffic information using airborne camera systems," ATLAS Center, Univ. Arizona, Tucson, Tech. Rep., 11-05-01.
[27] F.-Y. Wang, P. B. Mirchandani, and C. Y. Kuo, "Vista-vehicles with intelligent systems for transport automation," Arizona Dept. Transportation, Phoenix, Final Rep., 473(b), 2000.
[28] F.-Y. Wang and J. Sun, "Efficient extrinsic calibration of multiple camera systems and applications," PARCS, Univ. Arizona, Tucson, Tech. Rep. 0501-02, 2002.
[29] F.-Y. Wang, "A simple and analytical procedure for calibrating extrinsic camera parameters," *IEEE Trans. Robot. Automat.*, vol. 20, no. 1, pp. 121–124, Jan. 2004.
[30] G. Q. Wei and S. D. Ma, "A complete two-plane camera calibration method and experimental comparisons," in *Proc. Int. Conf. Computer Vision*, Berlin, Germany, 1993, pp. 439–446.
[31] Y. Yakmovsky and R. Cunningham, "A system for extracting three dimensional measurements from a stereo pair of TV cameras," *Comput. Graph. Image Process.*, vol. 7, pp. 195–210, 1978.
[32] Z. Zhang, "A flexible new technique for camera calibration," *IEEE Trans. Pattern Anal. Mach. Intell.*, vol. 22, no. 11, pp. 1330–1334, Nov. 2000.

Fei-Yue Wang (S'87–M'89–SM'94–F'03) received the B.S. degree in chemical engineering from the Qingdao University of Science and Technology, Qingdao, China, the M.S. degree in mechanics from Zhejiang University, Hangzhou, China, and the Ph.D. degree in electrical, computer, and systems engineering from the Rensselaer Polytechnic Institute, Troy, NY, in 1982, 1984, and 1990, respectively.

He jointed the University of Arizona, Tucson, in 1990 and became a Full Professor of systems and industrial engineering in 1999 and is currently the Director of the Program for Advanced Research in Complex Systems. In 1999, he founded the Intelligent Control and Systems Engineering Center at the Institute of Automation, Chinese Academy of Sciences, Beijing, China, under the support of the Outstanding Oversea Chinese Talents Program. Since 2002, he has been the Director of the Key Laboratory of Complex Systems and Intelligence Science, Chinese Academy of Sciences. He was the Editor-in-Chief of the *International Journal of Intelligent Control and Systems* from 1995 to 2000, Editor-in-Charge of *Series in Intelligent Control and Intelligent Automation* from 1996 to 2004, and he is currently the Editor-in-Charge of *Series in Complex Systems and Intelligence Science*. His current research interests include modeling, analysis, and control mechanism of complex systems; agent-based control systems; intelligent control systems; real-time embedded systems, application specific operating systems (ASOS); applications in intelligent transportation systems, intelligent vehicles and telematics, web caching and service caching, smart appliances and home systems, and network-based automation systems, and has published more than 200 books, book chapters, and papers in these areas since 1984 and received more than $20 million and over ¥50M RMB from NSF, DOE, DOT, NNSF, CAS, MOST, Caterpillar, IBM, HP, AT&T, GM, BHP, RVSI, ABB, and Kelon.

Dr. Wang is a member of Sigma Xi, ACM, AMSE, ASEE, and the International Council of Systems Engineering (INCOSE). He received the Caterpillar Research Invention Award with Dr. P. J. A. Lever in 1996 for his work in robotic excavation and the National Outstanding Young Scientist Research Award from the National Natural Science Foundation of China in 2001, as well as various industrial awards for his applied research from major corporations. He is an Associate Editor for the IEEE TRANSACTIONS ON INTELLIGENT TRANSPORTATION SYSTEMS, IEEE TRANSACTIONS ON SYSTEMS, MAN, AND CYBERNETICS, IEEE TRANSACTIONS ON ROBOTICS AND AUTOMATION, *IEEE Intelligent Systems*, and several other international journals. He is an elected member of IEEE SMC Board of Governors and the AdCom of the IEEE Nanotechnology Council, the Secretary and Vice President of IEEE Intelligent Transportation Systems Council, President-Elect of the IEEE Intelligent Transportation System Society, and Chair the Technical Committee on System Complexity of the Chinese Association of Automation. He was the Program Chair of the 1998 IEEE International Symposium on Intelligent Control, the 2001 IEEE International Conference on Systems, Man, and Cybernetics, Chair for Workshops and Tutorials for 2002 IEEE International Conference on Decision and Control (CDC), the General Chair of the 2003 IEEE International Conference on Intelligent Transportation Systems, Co-Program Chair of the 2004 IEEE International Symposium on Intelligent Vehicles (and he will be the General Chair for this same conference in 2005), and the General Chair of the IEEE 2005 International Conference on Networking, Sensing, and Control. He is the President of Chinese Association for Science and Technology, USA, and the Vice President and one of the major contributors of the American Zhu Kezhen Education Foundation, and a member of the Boards of Directors of five companies in information technology and automation.